

Improving the Morphological and Optical Properties of the CsPbBr₃ Films by PbI₂ Substitution for Efficient All-inorganic Perovskite Solar Cells

Fei ZHAO^{1*}, Yannan ZHANG¹, Yixin GUO²

¹ School of Photoelectric Engineering, Changzhou Institute of Technology, Changzhou, Jiangsu, 213032, China

² Department of Physics, Shanghai Normal University, Shanghai 200233, China

<http://doi.org/10.5755/j02.ms.39805>

Received 16 December 2024; accepted 13 February 2025

Wide band gap CsPbBr₃ perovskite solar cells are becoming one of the ideal candidates for top cells in tandem solar cells. Nevertheless, the defects in CsPbBr₃ film prepared by solution deposition method restrict the optoelectronic performance of perovskite solar cells. To solve this problem, a strategy of doping a trace amount of PbI₂ into CsPbBr₃ film synthesized by solution deposition is adopted, effectively increasing the average grain size of CsPbBr₃ film, decreasing its optical band gap, number of surface grain boundary defects and carrier recombination probability. Simultaneously, the PbI₂-doped CsPbBr₃ perovskite solar cells have been successfully prepared. The best conversion efficiency of the CsPbBr₃ cells with doping PbI₂ is 6.46 %, which is higher than the efficiency of the undoped CsPbBr₃ devices (5.00 %). This study offers a method for manufacturing highly efficient all-inorganic perovskite solar cells.

Keywords: doping PbI₂, CsPbBr₃, all-inorganic perovskite solar cells, optical band gap.

1. INTRODUCTION

Organic-inorganic hybrid perovskite solar cell (OIHPSC) has become one of the fastest developing photovoltaic technologies due to their comprehensive advantages such as high performance, low cost and solution processability [1–4]. The photoelectric conversion efficiency (PCE) of laboratory-scale organic-inorganic hybrid perovskite devices has increased from 3.8 % to 26 % [5], which is comparable to the efficiency of crystalline-silicon solar cells [6]. Nevertheless, they faces poor moisture, heat, and light stability [7, 8]. To address the aforementioned problems, all-inorganic perovskites (CsPbI₃, CsPbBr₃, CsPbIBr₂ and CsPbI₂Br) have been successfully synthesized [9–11]. Among these perovskites, the CsPbBr₃ based on a wide band gap (~2.3 eV) has attracted a lot of attention owing to its extraordinary humidity and thermal stability [12–14]. The advanced CsPbBr₃ cell displays an architecture of FTO/Nb₂O₅/CsPbBr₃/Carbon. Compared with the OIHPSC device, it significantly simplifies the manufacturing process and reduces costs [15]. Thus, more efforts are being made to enhance the efficiency of carbon-based CsPbBr₃ cell without sacrificing its stability.

The CsPbBr₃ film based on large grain size and low carrier recombination probability is a key factor for enhancing the efficiency of corresponding cell [16, 17]. Thus, the preparation of CsPbBr₃ film with large grain size and low carrier recombination probability is a prerequisite to improve device efficiency. To address this problem, the strategy of doping foreign ions into CsPbBr₃ perovskite lattice has been widely investigated. Through partially replacing Cs⁺ at the A-site with Li⁺, Na⁺, K⁺ and Rb⁺, the

grain sizes of CsPbI₂Br and CsPbBr₃ films can be increased to reduce charge recombination [15, 18]. In addition to the substitution at A-site, replacing partial Pb²⁺ at B-site with metal ions of the same or different valences can also have a passivation effect on the perovskite grains. Moreover, In³⁺, Al³⁺, Ca²⁺, Cd²⁺, Sr²⁺, Sn²⁺, Sm³⁺, Tb³⁺, Ho³⁺, Er³⁺ and Yb³⁺ in MAPbI₃ and CsPbBr₃ are respectively used to replace Pb²⁺, which increases grain size and reduces non-radiative recombination rate [19–24]. Compared with isoivalent substitution, heterovalent substitution can easily result in the formation of defect states [19, 25]. So far, there have been no reports on the effects of doping iodine ion on the structure and optoelectronic properties of CsPbBr₃ layer, as well as the photovoltaic property of corresponding devices.

In this study, doping PbI₂ can regulate the crystallinity of all-inorganic CsPbBr₃ film. Meanwhile, the CsPbBr₃ layer prepared by doping PbI₂ has a lower optical band gap, indicating the absorption of more solar light. In addition, the carrier recombination probability of the CsPbBr₃ layer is reduced after doping PbI₂. More importantly, the CsPbBr₃ cell based on PbI₂ achieves a champion efficiency of 6.46 %, which is much higher than 5.00 % for the undoped CsPbBr₃ cell. These findings suggest that doping PbI₂ offers a novel strategy for improving the quality of perovskite and the photovoltaic performance of all-inorganic CsPbBr₃ devices.

2. EXPERIMENTAL DETAILS

2.1. Device preparation

Before manufacturing solar cells, FTO glass was thoroughly ultrasonically rinsed with acetone, isopropanol, ethanol and deionized water. A uniform and dense Nb₂O₅

* Corresponding author: F. Zhao
E-mail: zhaofei@czu.cn

film was prepared on a clean FTO glass substrate by magnetron sputtering technology. The detailed information is as follows. The vacuum degree and substrate temperature for preparing Nb_2O_5 films are 3×10^{-4} Pa and 25°C , respectively. The power and time used for sputtering Nb_2O_5 are 130 W and 40 min, severally. The undoped CsPbBr_3 layer was manufactured via a multi-step solution deposition method. 1 M PbBr_2 solution in N,N-dimethylformamide (DMF) was deposited on the $\text{Nb}_2\text{O}_5/\text{FTO}$ at 2000 rpm for 30 s. Then, the PbBr_2 film was heated at 90°C for 30 min. Subsequently, 0.07 M CsBr methanol solution was deposited on the $\text{PbBr}_2/\text{Nb}_2\text{O}_5/\text{FTO}$ at 2000 rpm for 30 s. Afterwards, the CsBr film was annealed at 250°C for 5 min. The deposition and annealing times of CsBr are both 4 times. This successfully prepared an excellent CsPbBr_3 perovskite film. The PbI_2 -doped CsPbBr_3 perovskite was prepared by adding a certain proportion of PbI_2 to PbBr_2 solution. The rest of the process is the same as the above program. Eventually, a carbon electrode containing the area of 0.09 cm^2 was prepared on the $\text{CsPbBr}_2/\text{Nb}_2\text{O}_5/\text{FTO}$ through scraping carbon paste.

2.2. Characterizations

The morphology of the CsPbBr_3 layer was gained by employing a field-emission scanning electron microscope (SEM). The X-ray pattern of the CsPbBr_3 layer was recorded by utilizing an X-ray diffractometer (XRD). XPS spectroscopy can be used to analyze the elemental valence states of perovskite layers. The absorption spectra of different CsPbBr_3 layers were characterized to gain the optical band gaps of various CsPbBr_3 layers. The time-resolved PL (TRPL) spectra for CsPbBr_3 layers were conducted to obtain their carrier lifetimes. The photovoltaic parameters of CsPbBr_3 solar cells were obtained by J-V curves tested under AM 1.5 G ($100\text{ mW}/\text{cm}^2$).

3. RESULTS AND DISCUSSIONS

Fig. 1 a indicates the XRD patterns of different CsPbBr_3 films. The three typical peaks in all films appeared at 15.23° , 21.73° and 30.80° , corresponding to the (100), (110) and (200) crystal planes of the CsPbBr_3 [26]. In addition, there is a diffraction peak of 26.61° in both films, corresponding to FTO substrate [27]. No distinct impurity phase is found in all CsPbBr_3 films. For all CsPbBr_3 films, the diffraction peak intensity of the (110) crystal plane is higher than that of other crystal planes, indicating that the CsPbBr_3 films have undergone preferential growth. Meanwhile, the main peak intensity of the PbI_2 -doped CsPbBr_3 film is higher than that of the undoped CsPbBr_3 films, showing the higher crystalline quality of the CsPbBr_3 films with doping PbI_2 . Fig. 1b and c indicate the enlarged XRD spectra of (110) and (200) for the CsPbBr_3 without and with doping PbI_2 . The (110) diffraction peak of CsPbBr_3 layer shifts towards lower angle with the doping of PbI_2 , which attributes to the lattice expansion of perovskite induced by iodine ions [28]. Meanwhile, we found that the behavior of the (200) diffraction peak is consistent with that of the (110) diffraction peak. Fig. 1d indicates the Full Width at Half Maximum (FWHM) for (110) in different samples. Compared with the undoped CsPbBr_3 film, the FWHM of the PbI_2 -doped CsPbBr_3 film

is smaller. This suggests that the CsPbBr_3 films with doping PbI_2 have larger grain sizes.

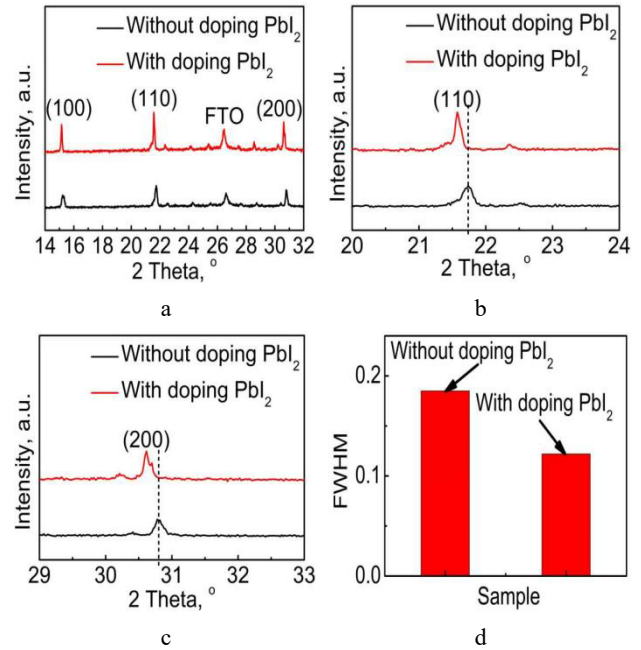


Fig. 1. a – XRD spectra of different CsPbBr_3 films; enlarged XRD spectra: b – (110); c – (200) for CsPbBr_3 without and with doping PbI_2 ; d – FWHM of (110) for different samples

Fig. 2 a indicates the XPS spectra (Br 3d) of various CsPbBr_3 films. The characteristic peak of CsPbBr_3 film shifts towards the direction of low binding energy after doping PbI_2 , demonstrating that iodine ions have been successfully doped into the CsPbBr_3 lattice. This result is consistent with the XRD analysis result. Fig. 2b indicates the XPS spectra (I 3d) of the PbI_2 -doped CsPbBr_3 film. From Fig. 2 b, it can be seen that the two characteristic peaks indicate that iodine ions are already present in CsPbBr_3 films.

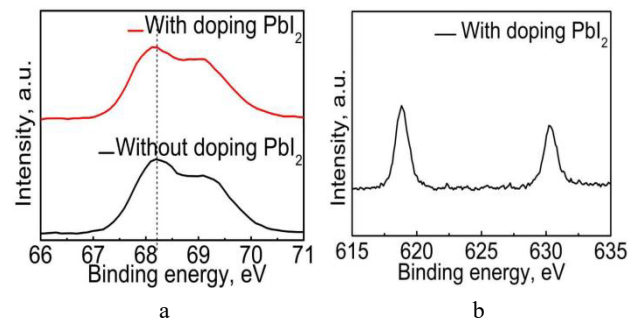


Fig. 2. a – XPS spectra (Br 3d) of various CsPbBr_3 films; b – XPS spectra (I 3d) of PbI_2 -doped CsPbBr_3 film

The SEM is commonly used to study the surface morphology of CsPbBr_3 layer. As seen in Fig. 3, there are a relatively uneven grains on the undoped CsPbBr_3 films. However, more uniform grains existed on the PbI_2 -doped CsPbBr_3 films. Clearly, the PbI_2 -doped CsPbBr_3 layer has a larger average grain size compared with the undoped CsPbBr_3 layer, showing that doping PbI_2 can promote the growth of CsPbBr_3 films. Additionally, we also observed that the CsPbBr_3 layers with doping PbI_2 have fewer grain boundaries. The aforementioned results are beneficial for

improving the photovoltaic performance of CsPbBr₃ cells [29].

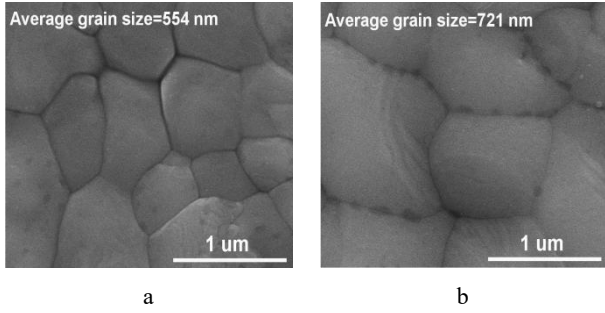


Fig. 3. Surface SEM images: a – undoped CsPbBr₃ film; b – PbI₂-doped CsPbBr₃ film

In order to investigate the optical absorption properties of different CsPbBr₃ layers, we conducted UV-VIS spectroscopy tests. As seen in Fig. 4, the light absorption of the PbI₂-doped CsPbBr₃ layer is stronger in comparison to that of the undoped CsPbBr₃ layer. The absorption enhancement may be attributed to the high crystallinity based on few grain boundaries for the PbI₂-doped CsPbBr₃ layer [30, 31]. In addition, the absorption edge of PbI₂-doped device exhibits a red shift phenomenon compared with undoped devices. This indicates that the optical band gap of PbI₂-doped devices is smaller. The above analysis results suggest that doping PbI₂ reduces the optical band gap of CsPbBr₃ layer. The reduction of the band gap can facilitate the more absorption of the photons for CsPbBr₃ cells, thereby generating many electron-hole pairs within the device. Ultimately, this effectively improves the short-circuit current density of the CsPbBr₃ device.

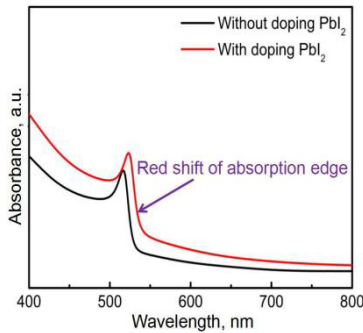


Fig. 4. Absorption spectra of undoped CsPbBr₃ film and PbI₂-doped CsPbBr₃ film

As shown in Fig. 5, TRPL measurements for different CsPbBr₃ samples grown on FTO substrates were conducted to investigate carrier dynamics and carrier lifetime. The carrier lifetime can be well obtained by Eq. 1:

$$f(t) = A_1 \exp\left(-\frac{t}{\tau_1}\right) + A_2 \exp\left(-\frac{t}{\tau_2}\right) + B, \quad (1)$$

where τ_1 and τ_2 reflect the slow and fast decay time constants, whilst A_1 , A_2 are the fractional amplitudes of τ_1 and τ_2 , separately. The average carrier lifetime (τ_{ave}) can be calculated to ascertain the entire recombination process, as shown by Eq. 2:

$$\tau_{ave} = \frac{\sum A_i \tau_i}{\sum A_i}. \quad (2)$$

The undoped CsPbBr₃ layer has an τ_{ave} value of 16.48 ns whereas an obviously improved τ_{ave} value of 36.03 ns can be detected for the PbI₂-doped CsPbBr₃ layer. The enhancement of the τ_{ave} value reveals that the carrier recombination probability and defect density in the CsPbBr₃ with doping PbI₂ are lower, which contributes to the process of photo-induced carrier transport and the final cell performance [32].

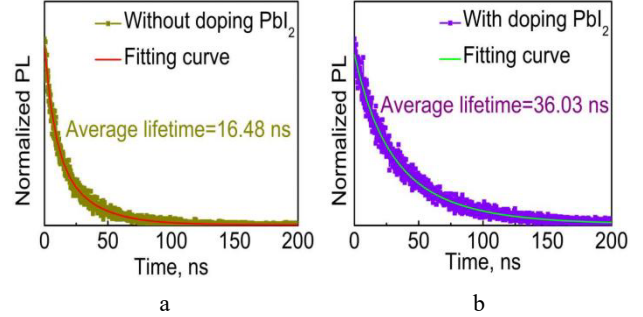


Fig. 5. TRPL spectra of a – undoped CsPbBr₃, b – PbI₂-doped CsPbBr₃ films deposited on FTO substrates

To investigate the photovoltaic performance of CsPbBr₃ cells, we first prepared a fully structured device. Our device consists of FTO glass substrate, Nb₂O₅ electronic transport layer, CsPbBr₃ absorption layer and carbon electrode. It is worth noting that there is no expensive hole transport layer in our device, which greatly saves the preparation cost of the device. After preparing the complete CsPbBr₃ device, we conducted J-V tests on different devices. Fig. 6 a and Table 1 exhibit the J-V characteristics and corresponding photovoltaic parameters of different CsPbBr₃ cells, respectively.

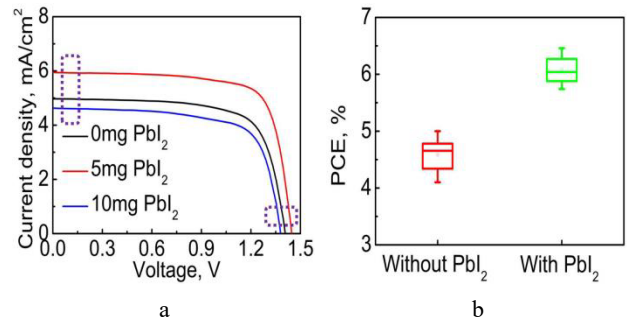


Fig. 6. a – J-V curves of CsPbBr₃ cell with different doping amount of PbI₂; b – average efficiency of CsPbBr₃ cell without and with doping PbI₂

Table 1. Photovoltaic parameters of CsPbBr₃ cell with different doping amount of PbI₂

Samples	V_{oc} , V	J_{sc} , mA/cm ²	FF , %	PCE , %
0 mg PbI ₂	1.406	4.97	71.59	5.00
5 mg PbI ₂	1.445	5.94	75.22	6.46
10 mg PbI ₂	1.379	4.63	70.51	4.50

The CsPbBr₃ cell with 0mg PbI₂ yields a relatively low efficiency of 5.00 %, coupled with an open-circuit voltage (V_{oc}) of 1.406 V, a short-circuit current density (J_{sc}) of 4.97 mA/cm² and a fill factor (FF) of 71.59 %. It is evident

that the photovoltaic performance of the solar cells with 5 mg PbI₂ outperform the unchanged devices. This marked improvement of J_{sc} , V_{oc} and FF can be attributed to enhanced crystallinity, reduced band gap, and decreased carrier recombination [33, 34]. The optimal incorporation of PbI₂ culminates in the champion cell, boasting an efficiency of 6.46 %, a V_{oc} of 1.445 V, a J_{sc} of 5.94 mA/cm², and an FF of 75.22 %. However, excessive incorporation of PbI₂ can reduce the photovoltaic performance of the device. Therefore, the optimal doping amount of PbI₂ is 5 mg. Fig. 6 b shows the average efficiency of the CsPbBr₃ cell without or with doping PbI₂. After incorporating PbI₂, the average efficiency of CsPbBr₃ cell (10 device) is 6.08 %, which shows the good repeatability of the device.

Fig. 7 a shows the Stability of CsPbBr₃ cell with doping PbI₂. The PbI₂-doped device is stored under approximately 80 % humidity and 25 °C. The PbI₂-doped device exhibits 97 % of initial efficiency, indicating superior stability of our device.

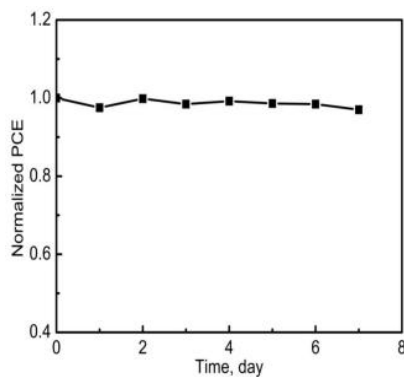


Fig. 7. Stability of CsPbBr₃ cell with doping PbI₂

According to previous reports [35], it has been found that iodine doping can improve the purity and phase stability of single crystal CsPbBr₃ films and help regulate the optical band gap. In our study, iodine doping can improve the crystallinity of polycrystalline CsPbBr₃ films, reduce their optical bandgap, and decrease their carrier recombination probability. More importantly, the efficiency of polycrystalline CsPbBr₃ solar cell has been significantly improved after iodine doping.

4. CONCLUSIONS

The PbI₂-doped all-inorganic CsPbBr₃ film and corresponding cell have been successfully prepared. The XRD and XPS tests indicate that iodine ions have been successfully doped into the lattice of CsPbBr₃ film. After PbI₂ incorporation, the crystallinity of CsPbBr₃ film is better and its optical band gap is smaller. Meanwhile, the PbI₂-doped CsPbBr₃ film possesses a less number of grain boundary defects and a lower probability of carrier recombination. Compared with the undoped CsPbBr₃ cell, the PbI₂-doped CsPbBr₃ cell achieves an outstanding efficiency of 6.46% with a V_{oc} of 1.445V, a J_{sc} of 5.94mA/cm² and a FF of 75.22%. This work provides a reasonable and effective process for the manufacturing of all-inorganic CsPbBr₃ cell.

Acknowledgements

This work was financed by the National Natural Science Foundation of China (No. 52402224 and No. 12304043).

REFERENCES

- Rong, Y., Hu, Y., Mei, A., Tan, H., Saidaminov, M.I., Seok, S.I., McGehee, M.D., Sargent, E.H., Han, H. Challenges for Commercializing Perovskite Solar Cells *Science* 361 2018: pp. eaat8235. <http://dx.doi.org/10.1126/science.aat8235>
- Yoo, J.J., Seo, G., Chua, M.R., Park, T.G., Lu, Y., Rotermund, F., Kim, Y.K., Moon, C.S., Jeon, N.J., Correa-Baena, J.P. Efficient Perovskite Solar Cells via Improved Carrier Management *Nature* 590 2021: pp. 587–593. <https://doi.org/10.1038/s41586-021-03285-w>
- Jeong, J., Kim, M., Seo, J., Lu, H., Ahlawat, P., Mishra, A., Yang, Y., Hope, M.A., Eickemeyer, F.T., Kim, M. Pseudo-halide Anion Engineering for α -FAPbI₃ Perovskite Solar Cells *Nature* 592 2021: pp. 381–385. <https://doi.org/10.1038/s41586-021-03406-5>
- Hossain, M.I., Saleque, A.M., Ahmed, S., Saidjafarzoda, I., Shahiduzzaman, M., Qarony, W., Knipp, D., Biyikli, N., Tsang, Y.H. Perovskite/perovskite Planar Tandem Solar Cells: A Comprehensive Guideline for Reaching Energy Conversion Efficiency Beyond 30% *Nano Energy* 79 2021: pp. 105400. <https://doi.org/10.1016/j.nanoen.2020.105400>
- Chen, J., Wu, Z., Chen, S., Zhao, W., Zhang, Y., Ye, W., Yang, R., Gong, L., Peng, Z., Chen, J. Light Harvesting and Carrier Transfer Enhancement of All-inorganic CsPbBr₃ Perovskite Solar Cells by Al-doped ZnO Nanorod Arrays *Materials Science in Semiconductor Processing* 174 2024: pp. 108186. <https://doi.org/10.1016/j.mssp.2024.108186>
- Xu, Y., Yan, C., Liang, H., Huang, S., Feng, P., Song, J. Large-scale Preparation of CsPbBr₃ Perovskite Quantum Dot/EVA Composite Adhesive Film by Melting for Crystal Silicon Solar Cell *Nanotechnology* 35 2024: pp. 175404. <https://doi.org/10.1088/1361-6528/ad2157>
- Dunfield, S.P., Bliss, L., Zhang, F., Luther, J.M., Zhu, K., Hest, M.F., Reese, M.O., Berry, J.J. From Defects to Degradation: A Mechanistic Understanding of Degradation in Perovskite Solar Cell Devices and Modules *Advanced Energy Materials* 10 2020: pp. 1904054. <https://doi.org/10.1002/aenm.201904054>
- Wei, J., Wang, Q., Huo, J., Gao, F., Gan, Z., Zhao, Q., Li, H. Mechanisms and Suppression of Photoinduced Degradation in Perovskite Solar Cells *Advanced Energy Materials* 11 2021: pp. 2002326. <https://doi.org/10.1002/aenm.202002326>
- Ouedraogo, N.A.N., Chen, Y., Xiao, Y.Y., Meng, Q., Han, C.B., Yan, H., Zhang, Y. Stability of All-inorganic Perovskite Solar Cells *Nano Energy* 67 2020: pp. 104249. <https://doi.org/10.1016/j.nanoen.2019.104249>
- Faheem, M.B., Khan, B., Feng, C., Farooq, M.U., Raziq, F., Xiao, Y., Li, Y. All-inorganic Perovskite Solar Cells: Energetics, Key Challenges, and Strategies toward Commercialization *ACS Energy Letters* 5

- 2020: pp. 290–320.
<http://doi.org/10.1021/acscenergylett.9b02338>
11. Tian, J., Xue, Q., Yao, Q., Li, N., Brabec, C.J., Yip, H.L. Inorganic Halide Perovskite Solar Cells: Progress and Challenges *Advanced Energy Materials* 10 2020: pp. 2000183.
<https://doi.org/10.1002/aenm.202000183>
 12. Yuan, B., Zhou, Y., Liu, T., Li, C., Cao, B. Extending the Absorption Spectra and Enhancing the Charge Extraction by the Organic Bulk Heterojunction for CsPbBr₃ Perovskite Solar Cells *ACS Sustainable Chemistry & Engineering* 11 2023: pp. 718–725.
<https://doi.org/10.1021/acssuschemeng.2c05859>
 13. Chai, W., Zhu, W., Zhang, Z., Liu, D., Ni, Y., Song, Z., Dong, P., Chen, D., Zhang, J., Zhang, C., Hao, Y. CsPbBr₃ Seeds Improve Crystallization and Energy Level Alignment for Highly Efficient CsPbI₃ Perovskite Solar Cells *Chemical Engineering Journal* 452 2023: pp. 139292.
<https://doi.org/10.1016/j.cej.2022.139292>
 14. Wang, Y., Tong, A., Wang, Y., Liang, K., Zhu, W., Wu, Y., Sun, W., Wu, J. Interfacial Modulation by Ammonium Salts in Hole Transport Layer Free CsPbBr₃ Solar Cells with Fill Factor over 86 % *Materials Today Chemistry* 40 2024: pp. 102228.
<https://doi.org/10.1016/j.mtchem.2024.102228>
 15. Lau, C.F.J., Deng, X., Ma, Q., Zheng, J., Yun, J.S., Green, M.A., Huang, S., Ho-Baillie, A.W.Y. CsPbI₂Br₂ Perovskite Solar Cell by Spray Assisted Deposition *ACS Energy Letters* 1 2016: pp. 573–577.
<http://doi.org/10.1021/acscenergylett.6b00341>
 16. Li, Y.N., Duan, J.L., Yuan, H.W., Zhao, Y.Y., He, B.L., Tang, Q.W. Lattice Modulation of Alkali Metal Cations Doped Cs_{1-x}R_xPbBr₃ Halides for Inorganic Perovskite Solar Cells *Solar RRL* 2018: pp. 1800164.
<https://doi.org/10.1002/solr.201800164>
 17. Zhang, L., Zhang, X.Z., Xu, X.X., Tang, J., Wu, J.H., Lan, Z. CH₃NH₃Br Additive for Enhanced Photovoltaic Performance and Air Stability of Planar Perovskite Solar Cells Prepared by Two-step Dipping Method *Energy Technology* 5 2017: pp. 1887–1894.
<https://doi.org/10.1002/ente.201700561>
 18. Guo, Y., Wang, Q., Saidi, W.A. Structural Stabilities and Electronic Properties of High-angle Grain Boundaries in Perovskite Cesium Lead Halides *Journal of Physical Chemistry C* 121 2017: pp. 1715–1722.
<https://doi.org/10.1021/acs.jpcc.6b11434>
 19. Nam, J.K., Chai, S.U., Cha, W., Choi, Y.J., Kim, W., Jung, M.S., Kwon, J., Kim, D., Park, J.H. Potassium Incorporation for Enhanced Performance and Stability of Fully Inorganic Cesium Lead Halide Perovskite Solar Cells *Nano Letters* 17 2017: pp. 2028–2033.
<https://doi.org/10.1021/acs.nanolett.7b00050>
 20. Duan, J.L., Zhao, Y.Y., Yang, X.Y., Wang, Y.D., He, B.L., Tang, Q.W. Lanthanide Ions Doped CsPbBr₃ Halides for HTM-free 10.14%-efficiency Inorganic Perovskite Solar Cell with An Ultrahigh Open-circuit Voltage of 1.594V *Advanced Energy Materials* 8 2018: pp. 1802346.
<https://doi.org/10.1002/aenm.201802346>
 21. Wang, Z.K., Li, M., Yang, Y.G., Hu, Y., Ma, H., Gao, X.Y., Liao, L.S. High Efficiency Pb-In Binary Metal Perovskite Solar Cells *Advanced Materials* 28 2016: pp. 6695–6703.
<https://doi.org/10.1002/adma.201600626>
 22. Wang, J.T.W., Wang, Z., Pathak, S., Zhang, W., deQuilettes, D.W., Rivarola, F.W.R., Huang, J., Nayak, P.K., Patel, J.B., Yusof, H.A.M., Vaynzof, Y., Zhu, R., Ramirez, G., Zhang, J., Ducati, C., Grovener, C., Johnston, M.B., Ginger, D.S., Nicholas, R.J., Snaith, H.J. An Efficient Perovskite Solar Cells by Metal Ion *Energy & Environmental Science* 9 2016: pp. 2892–2901.
<https://doi.org/10.1039/C6EE01969B>
 23. Swarnkar, A., Mir, W.J., Nag, A. Can B-Site Doping or Alloying Improve Thermal and Phase Stability of All-inorganic CsPbX₃ (X = Cl, Br, I) Perovskites *ACS Energy Letters* 3 2018: pp. 286–289.
<https://doi.org/10.1021/acscenergylett.7b01197>
 24. Guo, H., Pei, Y., Zhang, J., Cai, C., Zhou, K., Zhu, Y. Doping with SnBr₂ in CsPbBr₃ to Enhance the Efficiency of All-inorganic Perovskite Solar Cells *Journal of Materials Chemistry C* 7 2019: pp. 11234–11243.
<https://doi.org/10.1039/C9TC03359A>
 25. Zou, S., Liu, Y., Li, J., Liu, C., Feng, R., Jiang, F., Li, Y., Song, J., Zeng, H., Hong, M., Chen, X. Stabilizing Cesium Lead Halide Perovskite Lattice Through Mn(II) Substitution for Air-stable Light-emitting Diodes *Journal of the American Chemical Society* 139 2017: pp. 11443–11450.
<https://doi.org/10.1021/jacs.7b04000>
 26. Zhang, Z., Zhu, W., Han, T., Wang, T., Chai, W., Zhu, J., Xi, H., Chen, D., Lu, G., Dong, P., Zhang, J., Zhang, C., Hao, Y. Accelerated Sequential Deposition Reaction via Crystal Orientation Engineering for Low-temperature, High-efficiency Carbon-electrode CsPbBr₃ Solar Cells *Energy & Environmental Materials* 7 2024: pp. e12524.
<https://doi.org/10.1002/eem2.12524>
 27. Sun, H., Yu, L., Yuan, H., Zhang, J., Gan, X., Hu, Z., Zhu, Y. CoCl₂ as Film Morphology Controller for Efficient Planar CsPbI₂Br₂ Perovskite Solar Cells *Electrochimica Acta* 349 2020: pp. 136162.
<https://doi.org/10.1016/j.electacta.2020.136162>
 28. Atourki, L., Vega, E., Mollar, M., Kirou, H., Bouabid, K., Ihlal, A. Impact of Iodide Substitution on the Physical Properties and Stability of Cesium Lead Halide Perovskite Thin Films CsPbBr_{3-x}I_x (0 ≤ x ≤ 1) *Journal of Alloys and Compounds* 702 2017: pp. 404–409.
<http://dx.doi.org/10.1016/j.jallcom.2017.01.205>
 29. Liu, X., Tan, X., Liu, Z., Ye, H., Sun, B., Shi, T., Tang, Z., Liao, G. Boosting the Efficiency of Carbon-based Planar CsPbBr₃ Perovskite Solar Cells by a Modified Multistep Spin-coating Technique and Interface Engineering *Nano Energy* 56 2019: pp. 184–195.
<https://doi.org/10.1016/j.nanoen.2018.11.053>
 30. Zhu, W., Bao, C., Wang, Y., Li, F., Zhou, X., Yang, J., Lv, B., Wang, X., Yu, T., Zou, Z. Coarsening of One-step Deposited Organolead Triiodide Perovskite Films via Ostwald Ripening for High Efficiency Planar-heterojunction Solar Cells *Dalton Transactions* 45 2016: pp. 7856–7865.
<https://doi.org/10.1039/C6DT00900J>
 31. Zhao, F., Guo, Y., Tao, J., Li, Z., Jiang, J., Chu, J. Investigation of CsPbBr₃ Films with Controllable Morphology and Its Influence on the Photovoltaic Properties for Carbon-based Planar Perovskite Solar Cells *Applied Optics* 59 2020: pp. 5481–5486.
<https://doi.org/10.1364/AO.392404>
 32. Zhou, L., Sui, M., Zhang, J., Cao, K., Wang, H., Yuan, H., Lin, Z., Zhang, J., Li, P., Hao, Y., Chang, J. Tailored Buried Layer Passivation toward High-efficiency Carbon Based All-inorganic CsPbBr₃ Perovskite Solar Cell

Chemical Engineering Journal 496 2024: pp. 154043.
<https://doi.org/10.1016/j.ccej.2024.154043>

33. **Zhao, Y., Wang, Y., Duan, J., Yang, X., Tang, Q.** Divalent Hard Lewis Acid Doped CsPbBr₃ Films for 9.63%-efficiency and Ultra-stable All-inorganic Perovskite Solar Cells *Journal of Materials Chemistry A* 7 2019: pp. 6877–6882.
<https://doi.org/10.1039/C9TA00761J>
34. **Jiang, X., Geng, C., Yu, X., Pan, J., Zheng, H., Liang, C., Li, B., Long, F., Han, L., Cheng, Y., Peng, Y.** Doping with KBr to Achieve High-performance CsPbBr₃ Semitransparent Perovskite Solar Cells *ACS Applied Materials & Interfaces* 16 2024: pp. 19039–19047.
<https://doi.org/10.1021/acsami.4c02402>
35. **Sujith, P., Parne, S., Predeep, P.** Iodine Doping of CsPbBr₃: Toward Highly Stable and Clean Perovskite Single Crystals for Optoelectronic Applications *Philosophical Magazine* 103 2023: pp. 1213–1231.
<https://doi.org/10.1080/14786435.2023.21957>



© Zhao et al. 2026 Open Access This article is distributed under the terms of the Creative Commons Attribution 4.0 International License (<http://creativecommons.org/licenses/by/4.0/>), which permits unrestricted use, distribution, and reproduction in any medium, provided you give appropriate credit to the original author(s) and the source, provide a link to the Creative Commons license, and indicate if changes were made.